Cellulose (2022) 29:5235–5249
https://doi.org/10.1007/s10570-022-04606-6

ORIGINAL RESEARCH

Effect of a trace amount of deep eutectic solvents on the structure and optical properties of cellulose nanocrystal films

Xiaoyao Wei · Tao Lin · Hengli Du · Le Wang · Xuefeng Yin

Received: 12 November 2021 / Accepted: 20 April 2022 / Published online: 14 May 2022

Abstract Cellulose nanocrystal (CNC) suspensions can form chiral spiral structures because of their unique self-assembly characteristics, and their structures can be maintained in dried films. This makes CNC films possess iridescent and liquid crystal properties at the same time. However, neat CNC films are so fragile that they are not suitable for wide use. We first explored the influence of a new type of green plasticizer-deep eutectic solvent (formed by urea and choline chloride) on CNC composite films under different molar ratios and proportions. Deep eutectic solvents (DES) have attracted extensive attention in recent years due to their low cost, easy fabrication and no need for purification. Urea/choline chloride, as the original DES, can improve the apparent uniformity and smoothness of the film only by adding 1‰ of DES, maintaining the optical properties and structural stability of the CNC composite film while effectively reducing the brittleness of the film (the molar ratio of the CNC/DES film with the best performance is 2:1). When the amount of DES in the CNC aqueous suspension reaches 10‰, it will destroy the structure of the CNC, resulting in loss of the optical properties of the CNC/DES films. Different from the common small molecule plasticizers previously reported, the addition of DES not only increases the number of hydrogen bonds but also introduces charge force, which forms a network structure that synergistically improves the flexibility of CNC films.

Supplementary Information The online version contains supplementary material available at https://doi.org/10.1007/s10570-022-04606-6.

X. Wei · T. Lin · H. Du · L. Wang · X. Yin (✉)
College of Bioresources Chemical and Materials Engineering, Key Laboratory of Paper Based Functional Materials of China National Light Industry, Shaanxi Provincial Key Laboratory of Papermaking Technology and Specialty Paper Development, National Demonstration Center for Experimental Light Chemistry Engineering Education, Shaanxi University of Science and Technology, Xi'an 710021, Shaanxi, People's Republic of China
e-mail: yinxuefeng@sust.edu.cn

Graphical abstract

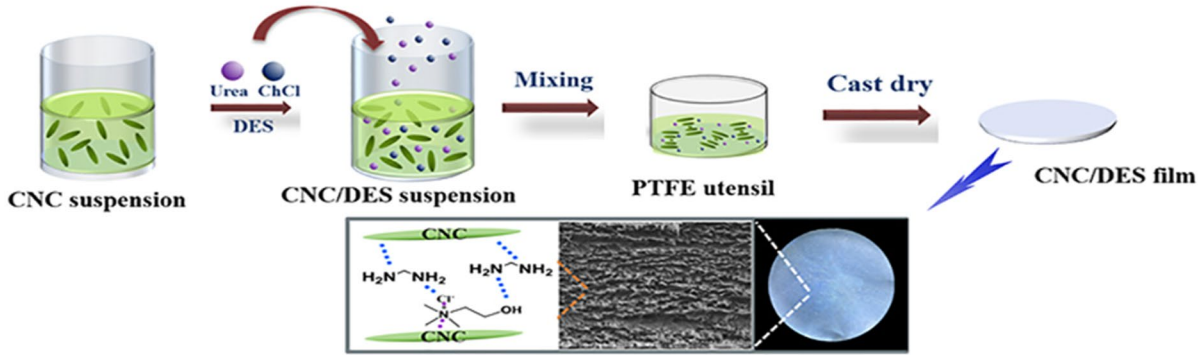

Keywords Cellulose nanocrystal film · Deep eutectic solvents · Urea · Choline chloride · Optical properties

Introduction

Cellulose nanocrystals (CNC) are a type of green biomaterial derived from natural cellulose, and they are sustainable, biodegradable and environmentally friendly (Dufresne 2013; Kelly et al. 2014; Klemm et al. 2005; Wang et al. 2019). When a CNC suspension reaches a certain critical concentration, it can self-assemble to form a liquid crystal with a left-handed spiral structure, and this unique structure can be maintained as a dried film (Gray 2016; Edgar and Gray 2001). The layered structure and periodic modulation of the refractive index make CNC films behave as photonic crystals. CNC films present iridescence and structural coloration; they can selectively reflect light with wavelengths that are in accordance with their pitch length, and it can be observed with the naked eye that the film is colored in a certain range (Wei et al. 2021a, b; Beck et al. 2011). CNC films also show strong left-handed circular polarized light. Because of these optical properties, this kind of optically active nanocellulose film has been widely studied in recent years and applied to sensors, decorative coatings and anti-counterfeiting agents (Bardet et al. 2015a, b; Gan et al. 2019; Zhao et al. 2020; Grey et al. 2019).

The high stiffness of the rod-like CNC makes the neat film inherently fragile, which limits its application value (Wang and Walther 2015). At present, there have been many studies on improving the flexibility of CNC films by adding various substances. A common method is to add polymers, such as polyethylene glycol (PEG) (Kelly et al. 2013; Yao et al. 2017), polyvinyl alcohol (PVA) (Bardet et al. 2015a, b; Zhu et al. 2016), waterborne polyurethane (WPU) (Wan et al. 2018) and polyvinylpyrrolidone (PVP) (Gao and Jin 2018), into CNC aqueous suspensions to maintain the optical performance and reduce the brittleness of CNC films. Another method is to add small molecules (glycerol, sorbitol, ethylene glycol, etc.) (He et al. 2018; Meng et al. 2020; Csiszár and Nagy 2017) as additives to the CNC aqueous suspension to construct a flexible iridescent CNC film. However, these methods are always accompanied by some problems. For example, the pitch of some composite films changes too much, and some bright additives will affect the color of the CNC films. Therefore, identifying a convenient method to improve the flexibility of CNC films without losing the optical response is very important.

Urea, the simplest small organic molecule, can be used as a plasticizer in green materials (Ma et al. 2004; Wang et al. 2014). We noticed that urea/choline chloride (ChCl), which was first discovered by Abbott et al. (2003) in 2003, is the most widely studied deep eutectic solvent (DES). DES are two-component or three-component eutectic mixtures of hydrogen bond acceptors (such as quaternary ammonium salt) and hydrogen bond donors (such as acrylamide, carboxylic acid, polyhydric alcohols), which has the characteristics of ionic liquids and organic solvents (Abbott

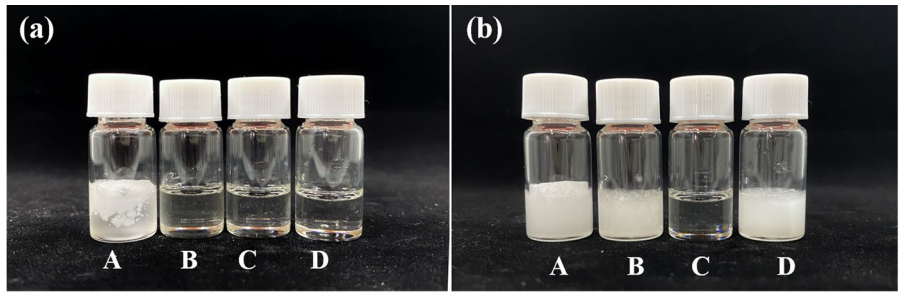

Fig. 1 Photographs of urea/choline chloride DES at different molar ratios. Solutions labeled A, B, C and D correspond to 1:2, 1:1, 2:1, 4:1. **a** DES solution at 90 ℃, **b** DES solution at 25 ℃

et al. 2003; Kareem et al. 2010; Choi et al. 2011). They are widely used in gas absorption (Sarmad et al. 2017; Altamash et al. 2016; Trivedi et al. 2016; Yang et al. 2017), electrochemistry (Steichen et al. 2011; Yang et al. 2011; Yue et al. 2012a, b), nanomaterials (Liao et al. 2008; Dong et al. 2010; Chirea et al. 2011) and organic synthesis (Imperato et al. 2005; Singh et al. 2011; Santi et al. 2012; Coulembier et al. 2012).

Currently, DES is used as a cost-effective green solvent in biomass-related research. Bi et al. (2013) used ChCl/1,4-butanediol as an extraction solvent to obtain flavonoids from *Chamaecyparis obtusa* leaves. Sirviö et al. (2020) pretreated cellulose with imidazole/choline chloride to obtain cellulose nanofibers. Ma et al. (2021a; 2021b) explored the delignification of poplar by using ethylene glycol-based and glycol-based DES. Most research on DES in CNC focuses on the use of DES instead of the traditional sulfuric acid method to prepare CNC particles.

To date, there have been a few reports about adding DES as plasticizers to green materials. Wang et al. (2015) plasticized regenerated cellulose film (RCF) using urea/choline chloride and showed it was an effective plasticizer. Zdanowicz and Johansson (2016) prepared two-component and three-component DES and studied their potential as starch plasticizers to prepare starch/DES films. Jakubowska et al. (2020) used chitosan and choline chloride-based DES with malonic acid (MA) to prepare biodegradable and non-toxic food-packaging materials. However, there are no reports on plasticizing CNC or CNC films with DES.

Herein, we first report the production of flexible CNC composite films with DES of different molar ratios (urea and choline chloride) as plasticizers. The effects of the DES content and composition ratio of the DES on the optical response and the flexibility of the CNC composite films were investigated. The added DES only accounted for 1‰ of the total amount and it functioned as a plasticizer that did not destroy the optical properties and improved the flexibility of the CNC films. The optical properties of the films were investigated by ultraviolet–visible spectroscopy (UV–vis) and polarized optical microscopy (POM). The morphological and structural features of the films were measured by X-ray diffraction spectroscopy (XRD), Fourier transform infrared spectroscopy (FTIR) and scanning electron microscopy (SEM).

Experimental section

Materials

Microcrystalline cellulose (MCC) powder was purchased from Shanghai Chineway Pharmaceutical Technology Co., Ltd. (Shanghai, China) as the raw material. The DES consisted of choline chloride and urea. Urea (≧ 99 wt%), glycerol (≧ 99 wt%) and sorbitol (≧ 98 wt%) were purchased from Damo Chemical Reagent Factory (Tianjin, China), and choline chloride (ChCl ≧ 98 wt%) was purchased from Shanghai Aladdin Biochemical Technology Co., Ltd. Ethanol absolute (CH_3CH_2OH ≧ 99.7 wt%), sulfuric acid (H_2SO_4 95–98 wt%) and sodium bicarbonate ($NaHCO_3$ ≧ 99.5 wt%) were purchased from Sinopharm Chemical Reagent Co., Ltd. (Nanjing, China). All of these reagents were used without further purification.

Methods

Preparation of the CNC suspension

CNC aqueous suspension was prepared from MCC by sulfuric acid hydrolysis (Bondeson et al. 2006; Wei et al. 2021a, b). In detail, 5 g MCC was hydrolyzed

in 64% sulfuric acid solution (88 mL) for 70 min at 50 °C. The reaction suspension was diluted 10 times with deionized (DI) water and dialyzed against DI water for several days until the pH was close to 6.0–7.0. Ultrasonic treatment was then carried out by an ultrasonic instrument (KQ3200DE, Kunshan ultrasonic instruments Co., Ltd., China) in an ice cooling bath at 200 W for 15 min to disperse the colloidal suspension. The solid content of the prepared CNC suspension was approximately 1.5 wt%.

Preparation of deep eutectic solvents

Different proportions of urea and choline chloride were sealed in a 50 mL flask with magnetic stirring and it was heated in an oil bath at 95 °C for 1 h (the mixture dissolved as a clear and viscous solution). The obtained solution was stored under vacuum at room temperature. The molar ratios of urea/choline chloride were 1:2, 1:1, 2:1 and 4:1 (Fig. 1).

Preparation of pure CNC and CNC/DES films

The neat CNC and CNC/DES films were all prepared from a CNC aqueous suspension with a concentration of 1.5 wt% and cast into a polytetrafluoroethylene (PTFE) disk with a diameter of 35 mm. The pure CNC film was dried at 25 °C for 4–7 days. The CNC/DES films were formed by adding various molar ratios of DES and prepared by the same method as the neat CNC film. The content of the DES solution in the CNC suspension was held at 1‰ (1/10000), while the molar ratio of urea/choline chloride varied from 1:2, 1:1, 2:1 and 4:1, and the corresponding films were marked as CNC/DES1, CNC/DES2, CNC/DES3 and CNC/DES4, respectively. The composite film with a urea/choline chloride molar ratio of 2:1 and DES content of 10‰ (10/10000) was marked as CNC/DES5. The CNC composite films prepared by adding 1‰ of urea, glycerin, sorbitol and ChCl into the CNC suspension were marked as CNC-U, CNC-G, CNC-S, and CNC-C. The 10‰ content of choline chloride was marked as CNC-C-10‰. The composite film prepared by separately adding 1‰ of urea and ChCl (molar ratio of 2:1) was marked as CNC-UC. The thickness and grammage of all of the films were approximately the same, 0.04 mm and 37.50 g/m^2, respectively.

Characterization

NMR

^{1}H NMR spectra were recorded on a Bruker AVANCE NEO (600 MHz ^{1}H), and ^{1}H chemical shifts are reported in ppm. The spectra were recorded in DMSO-d_6 as the solvent at room temperature.

Zeta potential, zeta-size and dispersity measurement

The zeta potential, zeta-size and Dispersity values of the aqueous suspension were measured by a Nano Zetasizer (Nano ZS90, Malvern, UK). The CNC and CNC/DES aqueous suspensions were diluted to 0.01 wt% at room temperature. Ultrasonic treatment was carried out with an ultrasonic bath (KQ3200DE, Kunshan ultrasonic instruments Co., Ltd., China) to obtain a homogeneous suspension before the measurement. The test was repeated 3 times for each sample, and the average value was calculated.

Atomic force microscopy

The morphology of the CNC/DES films was examined by atomic force microscopy (AFM, AFM5100, Agilent). AFM was operated in tapping mode. The CNC and CNC/DES films were affixed to mica sheets.

Scanning electron microscopy

Cross-sections of the films were observed by scanning electron microscopy (SEM, S4800, Rigaku). The film was broken under liquid nitrogen and then fixed on a vertical specimen holder. The sample was covered with a thin spray of gold before observation, and the acceleration voltage was 5 kV.

Polarized optical microscopy

The textures of the CNC/DES films were observed using polarized optical microscopy (POM, SMART-POL, OPTEC). (DM2700P, Germany).

Ultraviolet–visible spectroscopy

The ultraviolet–visible (UV–vis) spectra of the samples were measured with an ultraviolet–visible

spectrophotometer (Cary 5000, Agilent), and the wavelength ranged from 200 to 800 nm. The sample interval was 5 nm, and the scanning speed was 600 nm/min.

Fourier transform infrared spectroscopy

The Fourier transform infrared (FT-IR, Bruker, VERTEX 70) spectra of the films were used for testing the stress–strain, with a resolution of 2 cm^{-1} and a testing range of 400–4000 cm^{-1}. An average of 16 scans was reported.

X-ray diffraction

The X-ray diffraction (XRD) patterns of the samples were measured by an X-ray diffractometer (D8 Advance, Bruker) in the reflection mode. The diffracted intensity of the Cu Kα radiation was λ = 1.5406 Å. The scan rate of 0.02°min^{-1} along with a diffraction angle from 5° to 50° (2θ). The crystallinity index (CrI, %) was determined with the intensity ratio between the crystalline peak and the non-crystalline intensity obtained after the subtraction of the background signal according to the following Eq. (1):

$$CrI(\%) = \frac{I_{200} - I_{am}}{I_{200}} \times 100\% \quad (1)$$

where I_{200} is the maximum intensity of the lattice diffraction peak corresponding to the plane in the sample with the Miller indices (200) at angle of around 2θ = 22.5° and I_{am} represents diffraction of the non-crystalline phase, which is taken at an angle of around 2θ = 18° (Segal et al. 1959; French and Santiago Cintrón 2013; Borchani et al. 2015).

Stress–strain measurement

Before mechanical testing, all films were placed at 55% relative humidity and 27 °C for at least 24 h. The mechanical properties of the films were tested by a Servo material multifunctional high- and low-temperature control testing machine (AI-7000-AGD, Goodtechwill). Specimens were cut into 20 mm × 2 mm pieces. The stretching speed was 1 mm/min, and the

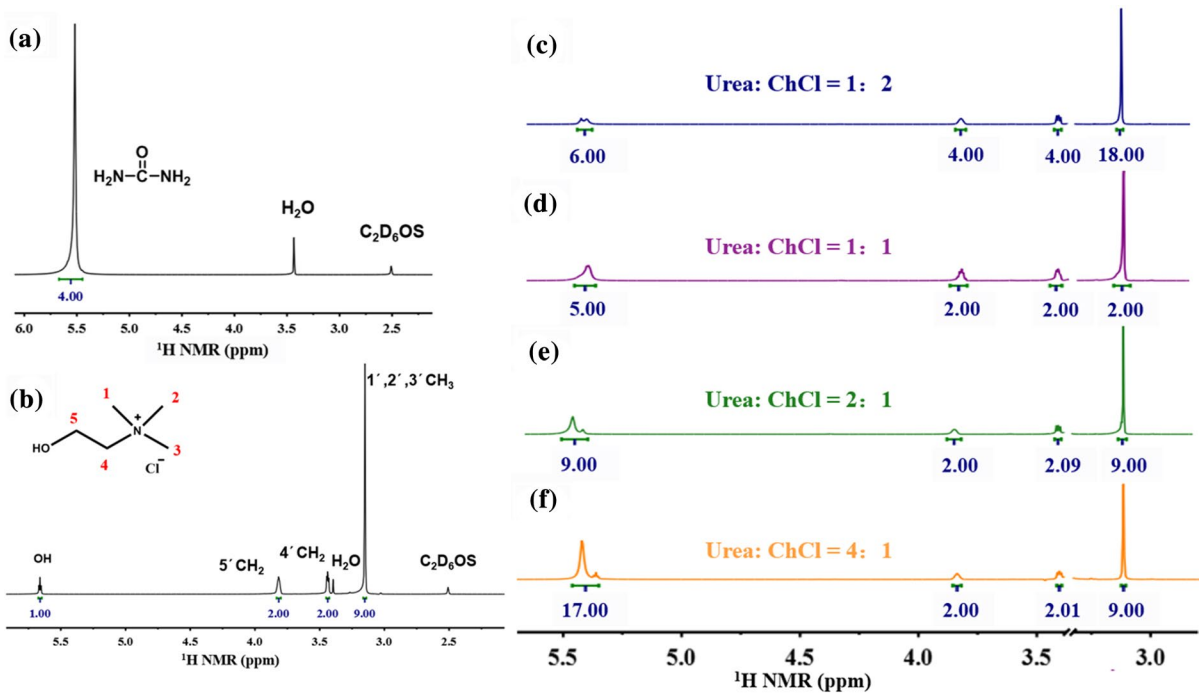

Fig. 2 ^{1}H NMR spectra of **a** urea, **b** choline chloride, **c** urea/ChCl = 1:2, **d** urea/ChCl = 1:1, **e** urea/ChCl = 2:1, and **f** urea/ChCl = 4:1

gauge length was 10 mm. At least four specimens were measured from each sample.

Results and discussion

Chemical composition of the DES and CNC/DES suspension

Figure 2 shows the ^{1}HNMR spectra of the urea, choline chloride and DES solutions with different molar ratios. In the ^{1}H NMR spectra, the solvent peak of DMSO-d_6 (C_2D_6OS) is at ~ 2.54 ppm, and the water peak is at ~ 3.33 ppm, which are marked in Fig. 2a and b. There are four H with the same chemical shift for the urea molecule, so only one peak appears at ~ 5.4 ppm, which can be seen in Fig. 2a. Figure 2b shows the structural formula of choline chloride, in which red numbers represent the serial numbers of carbon atoms. Choline chloride has four peaks in the ^{1}H NMR spectrum, which are ~ 3.1 ppm, ~ 3.5 ppm, ~ 4.0 ppm and ~ 5.6 ppm, and the H in carbon positions 1, 2 and 3 have the same chemical shift. Therefore, the number of H corresponding to the four peak positions from left to right is 9, 2, 2, 1. The molar ratios of urea/ChCl in DES solution are 1:2, 1:1, 2:1 and 4:1, and urea and choline chloride in DES both contain H at ~ 5.5 ppm, so the peaks will overlap. It can be seen from Fig. 2c–f that the chemical shifts of different H are the same as those of Fig. 2a and b, and the amount of hydrogen varies proportionally according to the molar ratio, showing that the urea and choline chloride in DES undergo no chemical reaction, only forming a simple physical mixture.

To explore the stability of the composite suspension, the zeta potential, zeta-size and Dispersity are shown in Fig. 3. A series of samples prepared under different molar ratios of urea/ChCl were measured, and the content of DES in the CNC aqueous suspension accounted for 1‰, except when the CNC/DES5 accounted for 10‰. All samples in neutral water showed a negative zeta potential. When the absolute

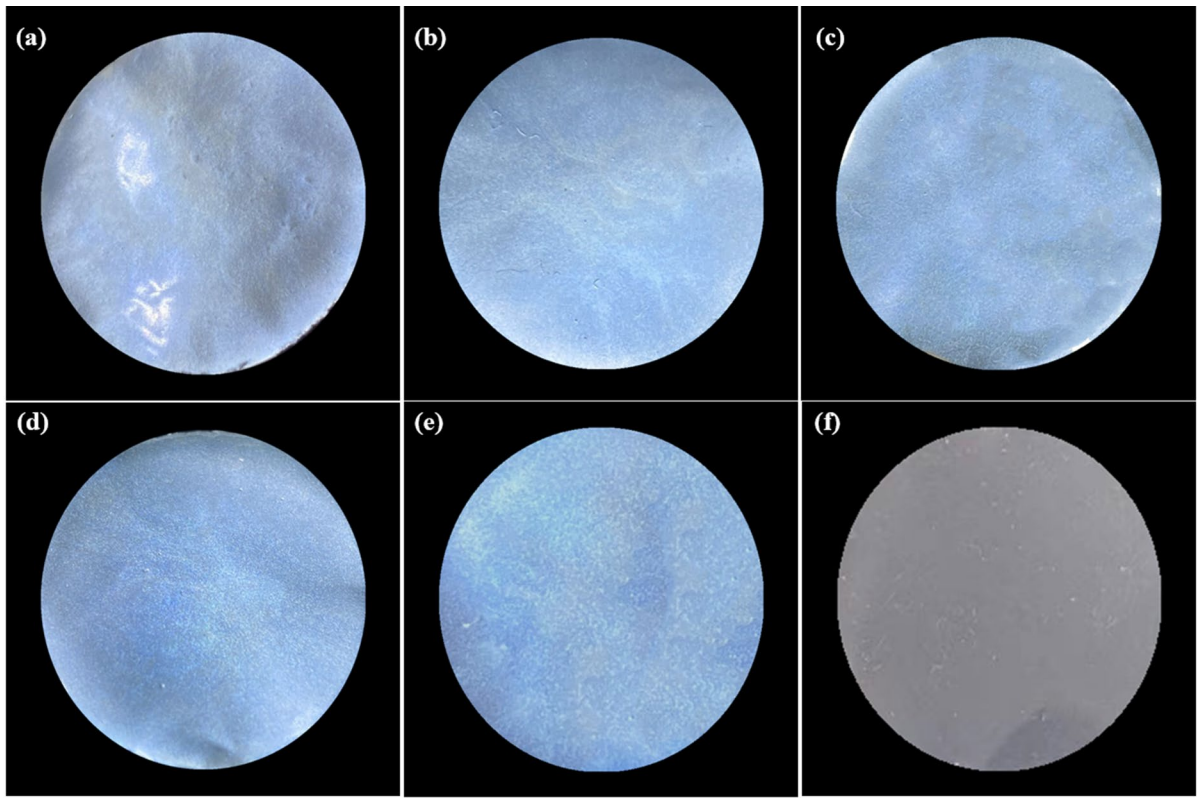

Fig. 3 Photographs of CNC and CNC/DES films. **a** Neat CNC film, CNC/DES films with different urea/ChCl molar ratios at a DES content of 1‰ **b** 1:2, **c** 1:1, **d** 2:1, **e** 4:1, **f** CNC/DES5 film with a urea/choline chloride molar ratio of 2:1 and DES content of 10‰

Table 1 Zeta potential, zeta-size and dispersity value of CNC and CNC/DES aqueous suspensions

Sample	CNC	CNC/DES1	CNC/DES2	CNC/DES3	CNC/DES4	CNC/DES5
Zeta potential (mV)	− 28.8 ± 1.7	− 33.8 ± 2.1	− 30 .8 ± 2.2	− 32.7 ± 0.9	− 30.2 ± 0.5	− 31.1 + 1.2
Zeta-size (nm)	85.6 ± 1.2	83.9 ± 0.4	84.1 ± 0.7	84.8 ± 0.8	83.8 ± 0.3	90.5 ± 0.9
Dispersity	0.433 ± 0.01	0.448 ± 0.02	0.427 ± 0.01	0.446 ± 0.02	0.440 ± 0.03	0.331 ± 0.02

value of the zeta potential of a suspension is greater than 30 mV, it can be said that the suspension is very stable (Kagaraeh et al. 2012). Table 1 shows that the absolute values of the zeta potential of the CNC composite suspension are all greater than 30 mV, and compared with neat CNC, the zeta potential fluctuates less and the value difference is not large (Fig. 3), which proves that the addition of DES does not affect the stability of the CNC aqueous suspension. As shown in Table 1, when the DES content is 1‰, the zeta-size differences among the CNC/DES1, CNC/DES2, CNC/DES3, CNC/DES4 and neat CNC aqueous suspensions are very small, the maximum difference is less than 2 nm, and the zeta-size curve is relatively stable. When the DES content reaches 10‰, the zeta-size increases to 90 nm, indicating that 1‰ DES will not affect the zeta-size of CNC, but 10‰ DES will. The Dispersity of all composition suspensions was kept at a value of 0.4, except 0.3 for CNC/DES5. Therefore, compared with Dispersity containing 1‰ DES, the composite suspension with 10‰ DES has poor dispersibility.

Optical properties of the CNC and CNC/DES films

Figure 3 shows photographs of the neat CNC film and CNC/DES films with a black board as the background. Under natural light, the CNC, CNC/DES1, CNC/DES2, CNC/DES3, and CNC/DES4 films all appear light blue. However, under the same conditions, the CNC/DES5 film cannot be observed with the naked eye, and it shows a transparent and colorless state. The CNC/DES films have iridescence when the content of DES is 1‰, but iridescence disappears when the content of DES is 10‰. It is speculated that DES with a content of 10‰ may

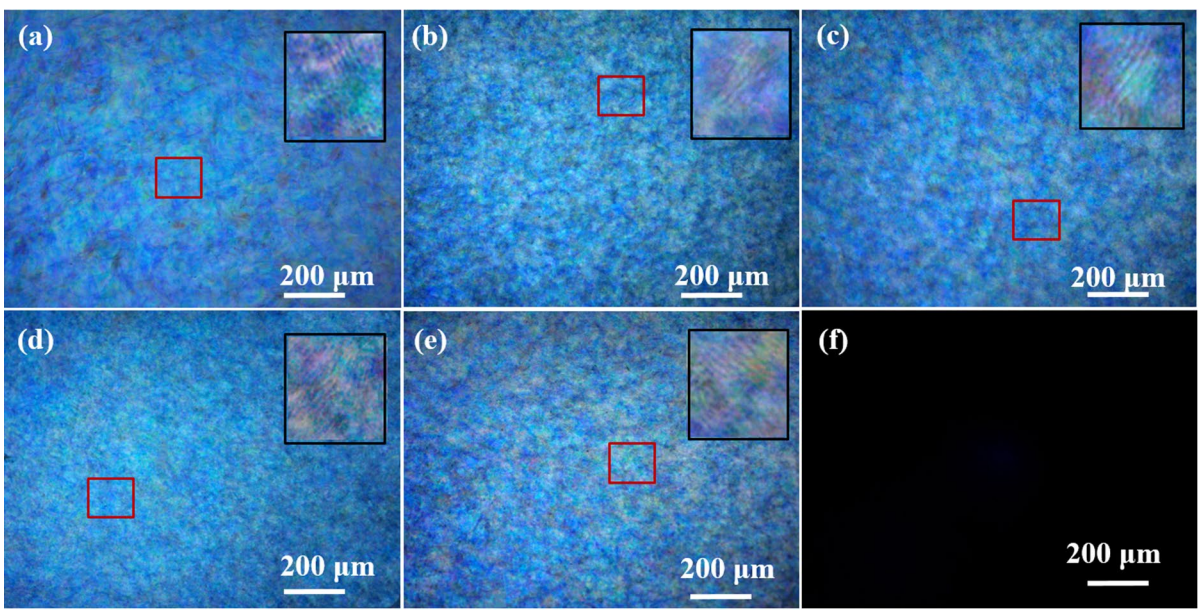

Fig. 4 POM images of CNC and CNC/DES films. **a** neat CNC, **b** CNC/DES1, **c** CNC/DES2, **d** CNC/DES3, **e** CNC/DES4, and **f** CNC/DES5. The inserted photo is a high-magnification image taken at the position marked by the red square

greatly increase the pitch value or directly destroy the formation of the CNC spiral structure. For the neat CNC film, a rough surface and poor uniformity are observed, but the surface of the CNC/DES films is relatively smooth. With the increase in the urea molar ratio in DES, the flatness was improved. This means that only 1‰ DES can effectively improve the appearance performance of CNC composite films. When the amount of DES in the CNC suspension is the same, with the change in molar ratio (the increase in urea molar ratio), the uniformity and smoothness of the films are improved differently. The CNC/DES3 film has the best flatness and uniformity, for which the molar ratio of urea/ChCl in the film is 2:1.

POM images of the neat CNC and CNC/DES films are shown in Fig. 4. Neat CNC, CNC/DES1, CNC/DES2, CNC/DES3, and CNC/DES4 films are a bright blue color, manifesting the characteristic birefringence phenomenon of the neat CNC film and CNC/DES films with 1‰ DES content. It is also obvious that there is no dramatic difference in the color of CNC/DES films with 1‰ DES content compared with neat CNC film. The "fingerprint" texture of the neat CNC film and CNC/DES films with 1‰ DES content can be seen in the inserted enlarged photos, except for CNC/DES5. The position corresponding to the enlarged photos is the position of the red box in the picture. The CNC/DES5 film is black under POM, and no pattern can be observed (Fig. 4f). After adding 1‰ content of DES into the composite film, and with the increase in the molar ratio of urea/ChCl (the increase in the urea molar ratio), the birefringence and "fingerprint" textures of the optical characteristics of the composite film are not affected. However, the CNC/DES5 film shows that when the DES content is as high as 10‰, the birefringent optical property of the CNC film will be destroyed.

Figure 5 shows the wavelength of the selective reflection of the neat CNC film and the CNC/DES films. With the increase in the molar ratio of urea/ChCl in DES, CNC/DES1, CNC/DES2 and CNC/DES3, they have similar wavelength curves of selective reflection. However, compared with neat CNC, the wavelengths of CNC/DES1, CNC/DES2 and CNC/DES3 selective reflection are slightly blue shifted to lower wavelengths, and their peak patterns are narrower. The peak shapes of the neat CNC film and the CNCDES4 film are similar, and the maximum reflection wavelengths are also similar. CNC/DES5 shows a line without a wavelength peak of selective reflection. This proves that 10‰ DES will also destroy the optical characteristics of the selective reflection of composite films.

Figure 5b shows the points corresponding to the maximum reflection wavelength in Fig. 5a. The maximum reflection wavelengths of the neat CNC film and the CNC/DES4 film are 411 nm and 423 nm, respectively, which are not much different. The maximum reflection wavelengths of the CNC/DES1, CNC/DES2 and CNC/DES3 films are also very similar, 394 nm, 397 nm and 394 nm, respectively. Because CNC/DES5 represents a straight line, there is no

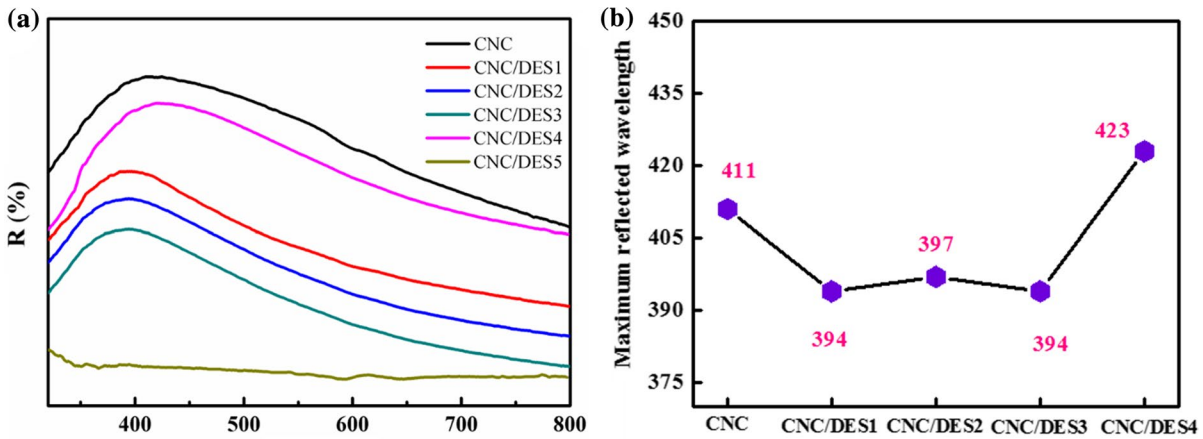

Fig. 5 **a** UV–Vis spectra of the CNC and CNC/DES films, **b** The maximum wavelength of selective reflection corresponding to CNC and CNC/DES films

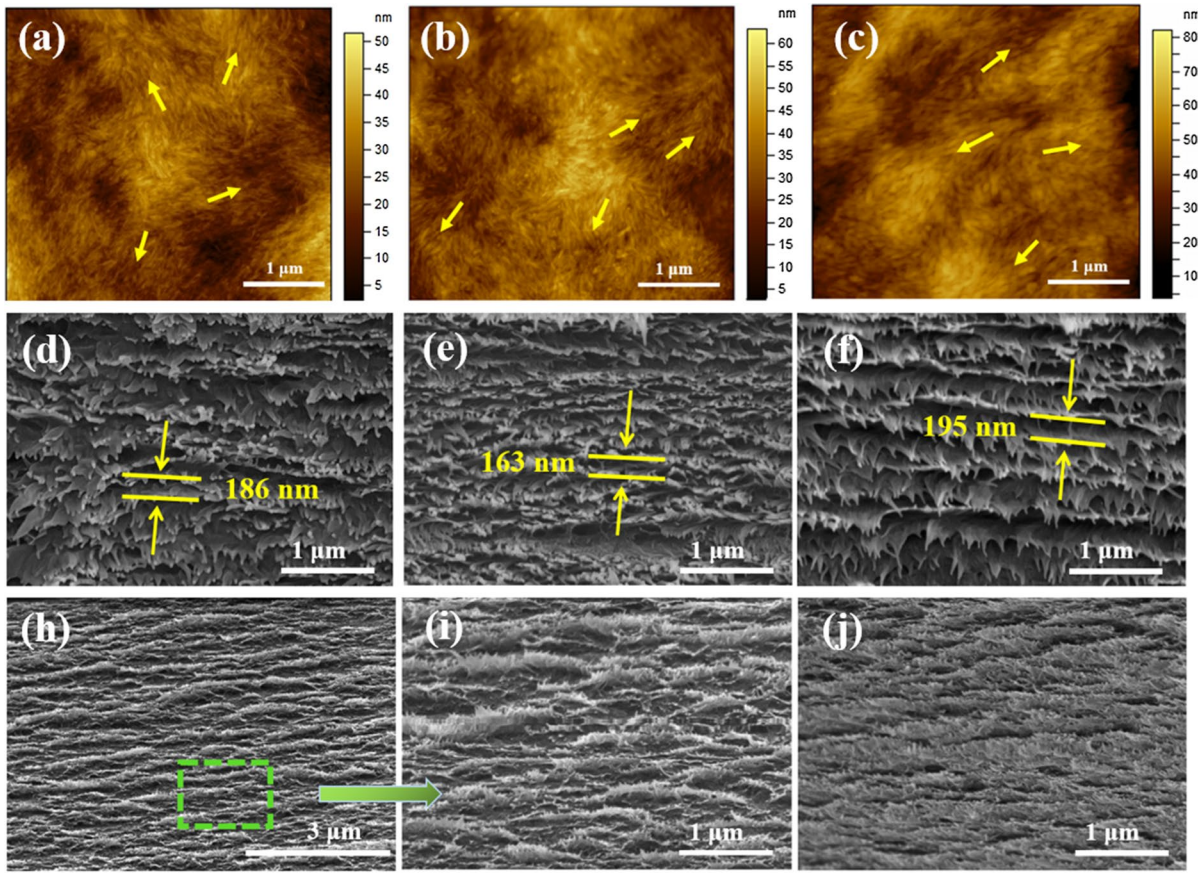

Fig. 6 AFM images of the **a** CNC film, **b** CNC/DES2 film, **c** CNC/DES4 film, SEM images of the cross-section of the **d** CNC film, **e** CNC/DES2 film, **f** CNC/DES4 film, **h** CNC/DES5 film with a scale bar of 3 μm, **i** partial enlargement of **h**, **j** CNC/DES5 film with scale bar of 1 μm

corresponding point in Fig. 5b. Therefore, compared with the neat CNC film, the optical properties of the CNC/DES films will be maintained when the content of DES is 1‰, and different molar ratios of urea/choline chloride will have different effects on the reflection wavelength. The phenomenon of a stable wavelength of selective reflection after adding DES is different from that of common plasticizers.

Morphology of the CNC and CNC/DES films

The morphologies of the plane surface of the CNC, CNC/DES2 and CNC/DES4 films are shown in Fig. 6a–c. The neat CNC film shows that the CNC rods have a directional arrangement at different positions on the plane, and the yellow arrows indicate the partial position of the directional arrangement. The CNC aqueous suspension has the characteristics of self-assembly to form a spiral structure, so the CNC rods will be aligned in one direction in this two-dimensional plane. The morphology of the CNC/DES2 and CNC/DES4 films is similar to that of the neat CNC film. However, although they have a directional orientation, the shape of the CNC rods is not as obvious as the neat CNC film shows, and the boundary state between the rods is weakened. This phenomenon may be because the addition of DES forms a network hydrogen bond structure within the CNC rods, thus filling the gap between the CNC rods and allowing the hydrogen bonds to more closely combine. Figure 6c shows that with the increase in the molar ratio of urea, this phenomenon becomes more obvious (Fig. S1 can be further proved), which may

be because urea provides more hydrogen bonds and increases the interaction force between them.

Figure 6d–f shows the morphologies of the cross-section surface of the CNC, CNC/DES2 and CNC/DES4 films. They all show a parallel layered structure, and the pitch (P) value can be obtained. The cross-sectional morphology of the CNC film is clean, the fragments appear locally, and the neat CNC film shows a P/2 = 186 nm. After adding DES, the CNC/DES2 and CNC/DES4 films have a more regular layered structure (P/2 = 163 nm and 195 nm, respectively), and the cross-sectional surface is uneven and has prominent parts parallel to the ridge and groove. With the increase in the molar ratio of urea/ChCl from 1:1 to 4:1, the layered structure seems to be more regular, uniform and more prominent. Compared with the neat CNC film, the change range of the pitch of the composite film is not large, and the change trend is consistent with the wavelength of the selective reflection.

Figure 6h and i present the same position of the CNC/DES5 film, but the magnification is different. Their layered structure is not obvious, and the arrangement is very messy and irregular, which can be seen more clearly from the higher magnification in Fig. 6i (the corresponding scale bar is 1 μm). Figure 6j shows another position of the CNC/DES5 film, showing the inconspicuous layered structure and the blocky and flat cross-section (the corresponding scale bar is 1 μm). The pitch of the structure can provide evidence for the wavelength of the selective reflection. These results indicate that CNC and DES with 1‰ content have good hydrogen bond interactions, and DES does not significantly affect the morphology and structure of CNC films produced by fracture. However, 10‰ DES will destroy the spiral structure of the CNC and cause it to lose its regular layered structure, resulting in a loss of optical performance.

Structural characterizations of the CNC and CNC/DES films

The XRD patterns of the neat CNC and CNC/DES films are shown in Fig. 7a. These films present the same diffraction peaks, and they all belong to cellulose I. The peaks are located at 14.9°, 16.5°and 22.7°, which correspond to the crystal planes (1–10), (110) and (200), respectively (Lin et al. 2012). The CrI of the pure CNC film is 87%, and the value of the composite films decreases slightly with the addition of DES. The CNC/DES2 and CNC/DES4 films CrI decreased to 84% (Calculation data about CrI can be found in the Table. S1). This demonstrated that no matter what the molar ratio of DES is added, it will not affect the crystal types of the CNC. However, DES will affect the crystalline region of cellulose and reduce its crystallinity.

Figure 7b illustrates the spectrograms of the neat CNC and CNC/DES films. The structural spectrograms of CNC/DES5 are not shown here because it has lost its optical activity. The absorption peak

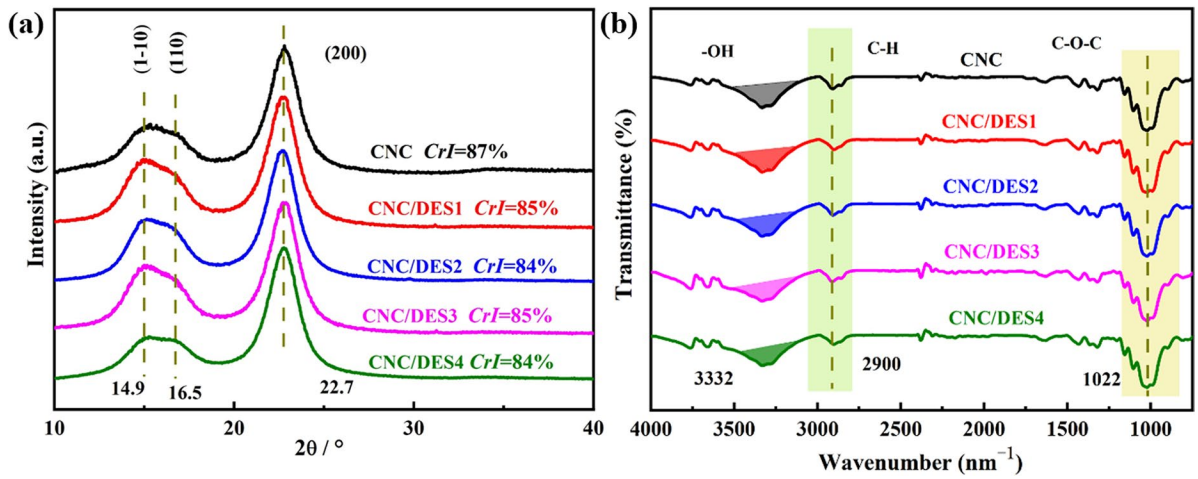

Fig. 7 **a** XRD of CNC and CNC/DES1-CNC/DES4 films, **b** FT-IR spectra of CNC/DES1-CNC/DES4 films

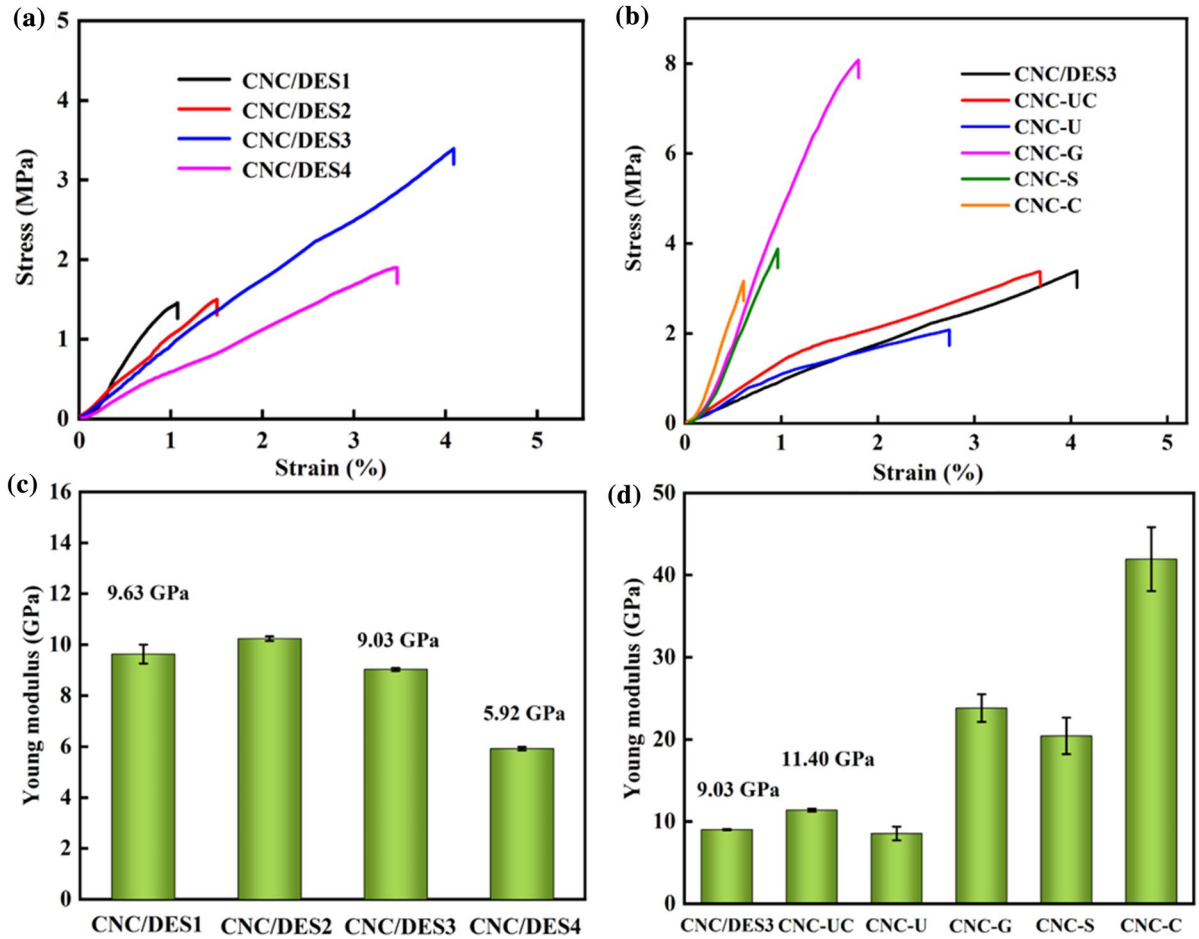

Fig. 8 Typical **a** stress–strain curves of CNC/DES films, **b** stress–strain curves of composite films, **c** Young modulus of CNC/DES films, and **d** Young modulus of composite films

at ~ 1022 cm^{-1} is the vibration of the C–O–C pyranose ring skeleton of cellulose nanocrystals (Jahan et al. 2011). The characteristic absorption peak in the green region at ~ 2900 cm^{-1} is the C–H stretching vibration (Lu et al. 2014). The absorption peak at ~ 1640 cm^{-1} is attributed to the stretching vibration of adsorbed water molecules (Lojewska et al. 2005). Comparing the stretching vibration peak of the characteristic -OH at ~ 3332 cm^{-1}, it can be seen that the peak positions of the neat CNC and CNC/DES films are the same, but the shapes of the peaks are slightly different with increasing molar ratios of urea (CNC/DES3 shows a relatively clear change). This may be due to the increase in the total number of hydrogen bonds formed between DES and CNC, and the added amount of DES is only 1‰, which makes the peak change of -OH at 3332 cm^{-1} not particularly obvious.

Mechanical properties of CNC/DES films

The mechanical properties of the resultant CNC/DES films with 1‰ content were evaluated via tensile testing at room temperature, and the stress–strain results are shown in Fig. 8a. The compared composite films of the stress–strain of urea/ChCl, urea, glycerol, sorbitol and ChCl are shown in Fig. 8b, and all of the composite films showed optical properties similar to those of DES/DES films (Fig. S2). Due to the severe cracking and brittleness of the neat CNC film, no measured value is obtained (Gray 2016). CNC/DES5 and CNC-C-10‰ lost their optical properties,

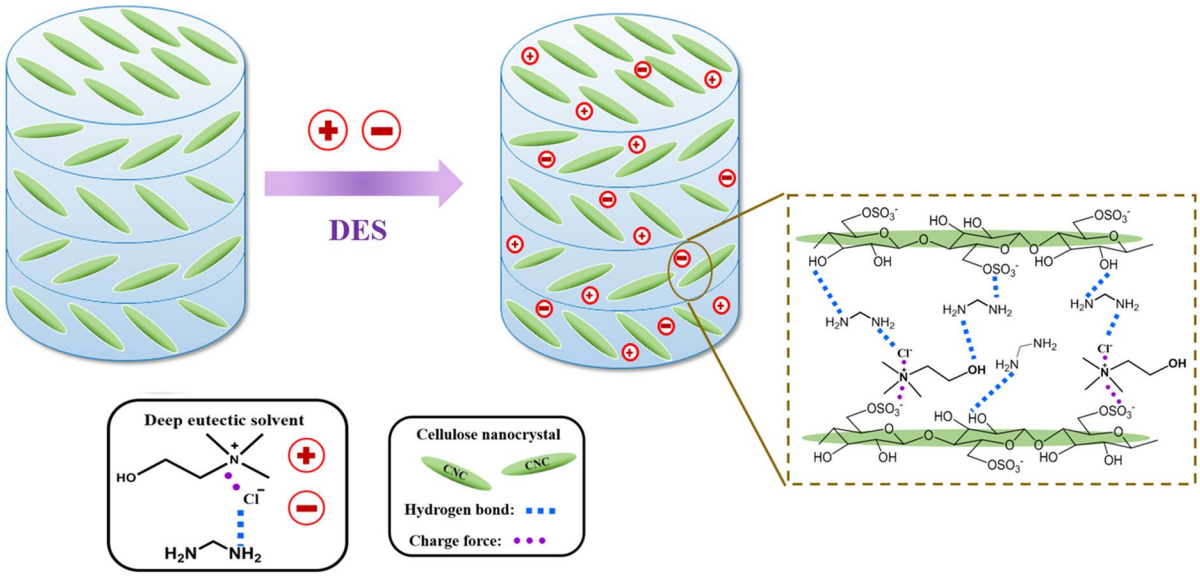

Scheme 1 Schematic diagram of the DES modification mechanism

so they are not tested for their mechanical properties. The Young's modulus of the CNC/DES film decreased with an increasing urea/ChCl molar ratio of DES, for which the lowest value of the CNC/DES4 film is 5.54 GPa, and the value of the CNC/DES3 film is also low (Fig. 8c). In addition, CNC/DES3 shows the best mechanical properties compared with other kinds of plasticizer composite films (Fig. 8b). The stress–strain curve of CNC-UC is similar to that of CNC/DES3, but CNC/DES3 shows a lower tensile strength and higher elongation at break (Fig. S3). The CNC-C film has the highest Young's modulus, while the CNC/DES3 and CNC-UC films have lower Young's modulus values of 9.03 GPa and 11.40 GPa, respectively. CNC/DES films possess enhanced mechanical properties due to hydrogen bonding and the charge force interaction network between the DES and CNC with sulfonic acid groups. The best mechanical performance is obtained when the urea/ChCl molar ratio in DES is 2:1 (CNC/DES3), and the tensile strength, elongation at break, and Young modulus are 3.39 MPa, 4.07%, and 9.03 GPa, respectively.

Mechanism of the CNC/DES films

Scheme 1 shows the interaction mechanism between CNC and DES. The DES consists of urea and choline chloride, in which choline chloride has positive and negative charges, and chlorine atoms will form hydrogen bonds with the hydrogen in urea. The red positive and negative charges in the scheme represent the composition of DES, and the green bars represent the cellulose nanocrystals. The green bars are arranged in the same direction on the plane, representing the layered structure of the CNC self-assembled spiral. There is no chemical reaction between DES and CNC, and two kinds of forces will appear in the structure of the composite film. The first is the electric charge force, which is due to the attraction between the negatively charged sulfate half-ester groups on CNC and the positively charged choline chloride in DES. Hydrogen bonding is the second kind of force. The chlorine atoms and nitrogen atoms in DES will form hydrogen bonds with free hydroxyl groups on the surface of the CNC, which competitively replaces the hydrogen bonds formed between the CNCs themselves, thus increasing the number of hydrogen bonds and improving the hydrogen bond interaction force. The electric charge force and hydrogen bond force cross each other to form a network structure, which can greatly improve the flexibility of the CNC films with a small amount of DES. With the increase in the urea/ChCl molar ratio, that is, the increase in the molar amount of urea, the total number of hydrogen bonds increases, but at the same time, the decrease in choline chloride also reduces the charge force.

Therefore, under the network of two forces, the force formed by CNC and the 2:1 molar ratio of urea/ChCl is the strongest, and its CNC/DES film shows the best optical and mechanical properties.

Conclusions

In summary, we have successfully used DES as a new type of plasticizer to obtain flexible CNC/DES films without significantly influencing their optical properties and structure. DES is prepared from urea and choline chloride in different molar ratios, and the optical properties and structure of the CNC/DES films remains stable, while the brittleness of the CNC/DES films is effectively improved by adding 1‰ DES. When the amount of DES in the CNC aqueous suspension is 10‰, it will destroy the spiral structure of CNC, resulting in the loss of optical properties of the CNC/DES films. Different from common small molecule plasticizers, DES competitively replaces the hydrogen bonds of CNC itself and creates more hydrogen bonds; moreover, the positive charges in DES will attract the negative charges of sulfonic acid groups on the surface of CNC obtained by the sulfuric acid method, which forms a network structure between DES and CNC in composite films. When the molar ratio of choline chloride/urea in DES is 2:1 and the addition amount is 1‰, the CNC/DES3 film shows good mechanical properties, with tensile strength, elongation at break and Young's modulus as follows: 38.71 MPa, 4.67%, and 8.13 GPa. Therefore, this is a green and effective method to maintain the optical properties of the film with a trace amount of addition, and the mechanical properties of the film is improved at the same time. This method has great application and development value for the combination and interaction of multiple additives added into CNC films at the same time.

Acknowledgments This work was supported by the Natural Science Basic Research Project in Shaanxi Province of China (2018JM2034) and the Science and Technology Research Project in Xianyang City, Shaanxi Province of China (2017k02-20).

Declarations

Conflict of interest The authors declare no competing financial interest.

Research involved in human and animal rights This article does not contain any studies with human or animal subjects performed by any of the authors.

References

Abbott AP, Capper G, Davies DL, Rasheed RK, Tambyrajah V (2003) Novel solvent properties of choline chloride/urea mixtures. Chem Commun 1:70–71. https://doi.org/10.1039/B210714G

Altamash T, Atilhan M, Aliyan A, Ullah R, García G, Aparicio S (2016) Insights into choline chloride–phenylacetic acid deep eutectic solvent for CO_2 absorption. RSC Adv 6(110):109201–109210. https://doi.org/10.1039/C6RA22312E

Bardet R, Belgacem N, Bras J (2015a) Flexibility and color monitoring of cellulose nanocrystal iridescent solid films using anionic or neutral polymers. ACS Appl Mater Interfaces 7(7):4010–4018. https://doi.org/10.1021/am506786t

Bardet R, Roussel F, Coindeau S, Belgacem N, Bras JJ (2015b) Engineered pigments based on iridescent cellulose nanocrystal films. Carbohyd Polym 122:367–375. https://doi.org/10.1016/j.carbpol.2014.10.020

Beck S, Bouchard J, Berry R (2011) Controlling the reflection wavelength of iridescent solid films of nanocrystalline cellulose. Biomacromol 12(1):167–172. https://doi.org/10.1021/bm1010905

Bi W, Tian M, Row KH (2013) Evaluation of alcohol-based deep eutectic solvent in extraction and determination of flavonoids with response surface methodology optimization. J Chromatogr A 1285:22–30. https://doi.org/10.1016/j.chroma.2013.02.041

Bondeson D, Mathew A, Oksman K (2006) Optimization of the isolation of nanocrystals from microcrystalline cellulose by acid hydrolysis. Cellulose 13:171–180. https://doi.org/10.1007/s10570-006-9061-4

Borchani KE, Carrot C, Jaziri M (2015) Untreated and alkali treated fibers from Alfa stem: effect of alkali treatment on structural, morphological and thermal features. Cellulose 22:1577–1589. https://doi.org/10.1007/s10570-015-0583-5

Chirea M, Freitas A, Vasile BS, Ghitulica C, Pereira CM, Silva F (2011) Gold nanowire networks: synthesis, characterization, and catalytic activity. Langmuir 27(7):3906–3913. https://doi.org/10.1021/la104092b

Choi YH, Spronsen JV, Dai Y, Verberne M, Hollmann F, Arends IWCE, Witkamp G, Verpoorte R (2011) Are natural deep eutectic solvents the missing link in understanding cellular metabolism and physiology? Plant Physiol 156(4):1701–1705. https://doi.org/10.1104/pp.111.178426

Coulembier O, Lemaur V, Josse T, Minoia A, Dubois P (2012) Synthesis of poly(L-lactide) and gradient copolymers from a L-lactide/trimethylene carbonate eutectic melt. Chem Sci 3:723–726. https://doi.org/10.1039/C2SC00590E

Csiszár E, Nagy S (2017) A comparative study on cellulose nanocrystals extracted from bleached cotton and flax and used for casting films with glycerol and sorbitol plasticisers. Carbohydr Polym 174:740–749. https://doi.org/10.1016/j.carbpol.2017.06.103

Dong J, Hsu Y, Wong D, Lu S (2010) Growth of ZnO nanostructures with controllable morphology using a facile green antisolvent method. J Phys Chem C 114(19):8867–8872. https://doi.org/10.1021/jp102396f

Dufresne A (2013) Nanocellulose: a new ageless bionanomateria. Mater Today 16(6):220–227. https://doi.org/10.1016/j.mattod.2013.06.004

Edgar CD, Gray DG (2001) Induced circular dichroism of chiral nematic cellulose films. Cellulose 8:5–12. https://doi.org/10.1023/A:1016624330458

French AD, Santiago Cintrón M (2013) Cellulose polymorphy, crystallite size, and the Segal Crystallinity Index. Cellulose 20:583–588. https://doi.org/10.1007/s10570-012-9833-y

Gan L, Feng N, Liu S, Zheng S, Li Z, Huang J (2019) Assembly-induced emission of cellulose nanocrystals for hiding information. Part Part Syst Charact 36:1800412. https://doi.org/10.1002/ppsc.201800412

Gao Y, Jin Z (2018) Iridescent chiral nematic cellulose nanocrystal/polyvinylpyrrolidone nanocomposite films for distinguishing similar organic solvents. ACS Sustain Chem Eng 6:6192–6202. https://doi.org/10.1021/acssuschemeng.7b04899

Gray DG (2016) Recent advances in chiral nematic structure and iridescent color of cellulose nanocrystal films. Nanomaterials 6(11):213. https://doi.org/10.3390/nano6110213

Grey P, Fernandes SN, Gaspar D, Fortunato E, Martins R, Godinho MH, Pereira L (2019) Field-effect transistors on photonic cellulose nanocrystal solid electrolyte for circular polarized light sensing. Adv Funct Mater 29:1805279.1-1805279.8. https://doi.org/10.1002/adfm.201805279

He Y, Zhang Z, Xue J (2018) Biomimetic optical cellulose nanocrystal films with controllable iridescent color and environmental stimuli-responsive chromism. ACS Appl Mater Interfaces. https://doi.org/10.1021/acsami.7b18440

Imperato G, Eibler E, Niedermaier J, Konig B (2005) Low-melting sugar–urea–salt mixtures as solvents for Diels-Alder reactions. Chem Commun 9:1170–1172. https://doi.org/10.1039/b414515a

Jahan MS, Saeed A, He Z, Ni Y (2011) Jute as raw material for the preparation of microcrystalline cellulose. Cellulose 18:451–459. https://doi.org/10.1007/s10570-010-9481-z

Jakubowska E, Gierszewska M, Nowaczyk J, Olewnik-Kruszkowska E (2020) Physicochemical and storage properties of chitosan-based films plasticized with deep eutectic solvent. Food Hydrocolloids 108:106007. https://doi.org/10.1016/j.foodhyd.2020.106007

Kagaraeh H, Ahmad I, Abullah I, Dufresne A, Zainudin SY, Sheltami RM (2012) Efects of hydrolysis conditions on the kenaf bast fibers. Cellulose 19(3):855–866. https://doi.org/10.1007/s10570-012-9684-6

Kareem MA, Mjalli FS, Hashim MA, Alnashef IM (2010) Phosphonium-based ionic liquids analogues and their physical properties. J Chem Eng Data 55(11):4632–4637. https://doi.org/10.1021/je100104v

Kelly JA, Yu M, Hamad WY, Maclachlan MJ (2013) Large, crack-free freestanding films with chiral nematic structures. Adv Opt Mater 1(4):295–299. https://doi.org/10.1002/adom.201300015

Kelly JA, Giese M, Shopsowitz KE, Hamad WY, Maclachlan MJ (2014) The development of chiral nematic mesoporous materials. Acc Chem Res 47(4):1088–1096. https://doi.org/10.1021/ar400243m

Klemm D, Heublein B, Fink HP, Bohn A (2005) Cellulose: fascinating biopolymer and sustainable raw material. Angew Chem Int Ed 44(22):3358–3393. https://doi.org/10.1002/anie.200460587

Liao H, Jiang Y, Zhou Z, Chen S, Sun S (2008) Shape controlled synthesis of gold nanoparticles in deep eutectic solvents for studies of structure-functionality relationships in electrocatalysis. Angew Chem 120(47):9240–9243. https://doi.org/10.1002/ange.200803202

Lin N, Huang J, Chang P (2012) Surface acetylation of cellulose nanocrystal and its reinforcing function in poly (lactic acid). Carbohyd Polym 83:1834–1842. https://doi.org/10.1016/j.carbpol.2010.10.047

Lojewska J, Miskowiec P, Lojewski T, Pronewicz LM (2005) Cellulose oxidative and hydrolysis degradation: in situ FTIR approach. Polym Degrad Stab 88(3):512–520. https://doi.org/10.1016/j.polymdegradstab.2004.12.012

Lu Q, Tang L, Lin F, Wang S, Chen Y, Chen X, Huang B (2014) Preparation and characterization of cellulose nanocrystals via ultrasonication-assisted $FeCl_3$-catalyzed hydrolysis. Cellulose 21:3497–3506. https://doi.org/10.1007/s10570-014-0376-2

Ma X, Yu J, Feng J (2004) Urea and formamide as a mixed plasticizer for thermoplastic starch. Polym Int 53(11):1780–1785. https://doi.org/10.1002/pi.1580

Ma C, Gao X, Peng X, Gao Y, Liu J, Wen J, Yuan T (2021a) Microwave-assisted deep eutectic solvents (DES) pretreatment of control and transgenic poplars for boosting the lignin valorization and cellulose bioconversion. Ind Crops Prod 164:113415. https://doi.org/10.1016/j.indcrop.2021.113415

Ma C, Xu L, Zhang C, Guo K, Yuan T, Wen J (2021b) A synergistic hydrothermal-deep eutectic solvent (DES) pretreatment for rapid fractionation and targeted valorization of hemicelluloses and cellulose from poplar wood. Biores Technol 341:125828. https://doi.org/10.1016/j.biortech.2021.125828

Meng Y, Cao Y, Ji H, Chen J, He Z, Long Z, Dong C (2020) Fabrication of environmental humidity-responsive iridescent films with cellulose nanocrystal/polyols. Carbohyd Polym 240:116281. https://doi.org/10.1016/j.carbpol.2020.116281

Santi VD, Cardellini F, Brinchi L, Germani R (2012) Novel broensted acidic deep eutectic solvent as reaction media for esterification of carboxylic acid with alcohols. ChemInform 53(52):5151–5155. https://doi.org/10.1002/chin.201252059

Sarmad S, Mikkola J, Ji X (2017) Carbon dioxide capture with ionic liquids and deep eutectic solvents: a new generation of sorbents. Chemsuschem 10(2):324–352. https://doi.org/10.1002/cssc.201600987

Segal L, Creely JJ, Martin AE, Conrad CM (1959) An empirical method for estimating the degree of crystallinity of native cellulose using the X-ray diffractometer. Text Res J 29(10):786–794. https://doi.org/10.1177/004051755902901003

Singh B, Lobo H, Shankarling G (2011) Selective N-Alkylation of aromatic primary amines catalyzed by bio-catalyst or deep eutectic solvent. Catal Lett 141(1):178–182. https://doi.org/10.1007/s10562-010-0479-9

Sirviö JA, Hyypiö K, Asaadi S, Junka K, Liimatainen H (2020) High-strength cellulose nanofibers produced via swelling pretreatment based on a choline chloride–imidazole deep eutectic solvent. Green Chem 22:1763–1775. https://doi.org/10.1039/C9GC04119B

Steichen M, Thomassey M, Siebentritt S, Dale PJ (2011) Controlled electrodeposition of cu-ga from a deep eutectic solvent for low cost fabrication of cugase2 thin film solar cells. Phys Chem Chem Phys 13(10):4292–4302. https://doi.org/10.1039/c0cp01408g

Trivedi TJ, Ji H, Lee HJ, You K, Choi J (2016) Deep eutectic solvents as attractive media for CO_2 capture. Green Chem 18(9):2834–2842. https://doi.org/10.1039/c5gc02319j

Wan H, Li X, Zhang L, Li X, Liu P, Jiang Z, Yu Z (2018) Rapidly responsive and flexible chiral nematic cellulose nanocrystal composites as multifunctional rewritable photonic papers with eco-friendly inks. ACS Appl Mater Interfaces 10:5918–5925. https://doi.org/10.1021/acsami.7b19375

Wang B, Walther A (2015) Self-assembled, iridescent, crustacean-mimetic nanocomposites with tailored periodicity and layered cuticular structure. ACS Nano 9(11):10637–10646. https://doi.org/10.1021/acsnano.5b05074

Wang J, Cheng F, Zhu P (2014) Structure and properties of urea-plasticized starch films with different urea contents. Carbohydr Polym 101:1109–1115. https://doi.org/10.1016/j.carbpol.2013.10.050

Wang S, Peng X, Zhong L, Jing S, Cao X, Lu F, Sun R (2015) Choline chloride/urea as an effective plasticizer for production of cellulose films. Carbohydr Polym 117:133–139. https://doi.org/10.1016/j.carbpol.2014.08.113

Wang Z, Li N, Zong L, Zhang J (2019) Recent advances in vacuum assisted self-assembly of cellulose nanocrystals. Curr Opin Solid State Mater Sci 23(3):142–148. https://doi.org/10.1016/j.cossms.2019.03.001

Wang B, Walther A (2015) Self-assembled, iridescent, crustacean-mimetic nanocomposites with tailored periodicity and layered cuticular structure. ACS Nano 9(11):10637–10646. https://doi.org/10.1021/acsnano.5b05074

Wei X, Lin T, Duan M, Du H, Yin X (2021a) Cellulose nanocrystal-based liquid crystal structures and the unique optical characteristics of cellulose nanocrystal films. BioResources 16:2116–2137. https://doi.org/10.15376/biores.16.1.Wei

Wei X, Lin T, Wang L, Yin X (2021b) Effect of a limited amount of D-sorbitol on pitch and mechanical properties of cellulose nanocrystal films. Curr Comput-Aided Drug Des 11(11):1324. https://doi.org/10.3390/cryst11111324

Yang H, Guo X, Birbilis N, Wu G, Ding W (2011) Tailoring nickel coatings via electrodeposition from a eutectic-based ionic liquid doped with nicotinic acid. Appl Surf Sci 257(21):9094–9102. https://doi.org/10.1016/j.apsusc.2011.05.106

Yang D, Han Y, Qi H, Wang Y, Sheng D (2017) Efficient absorption of SO_2 by EmimCl-EG deep eutectic solvents. ACS Sustain Chem Eng 5(8):6382–6386. https://doi.org/10.1021/acssuschemeng.7b01554

Yao K, Meng Q, Bulone V, Zhou Q (2017) Flexible and responsive chiral nematic cellulose nanocrystal/poly (ethylene glycol) composite films with uniform and tunable structural color. Adv Mater 29(28):1701323.1-1701323.8. https://doi.org/10.1021/10.1002/adma.201701323

Yue D, Jia Y, Ying Y, Sun J, Yan J (2012a) Structure and electrochemical behavior of ionic liquid analogue based on choline chloride and urea. Electrochim Acta 65(Supplement C):30–36. https://doi.org/10.1016/j.electacta.2012.01.003

Yue Y, Zhou C, French AD, Xia G, Han G, Wang Q, Wu Q (2012b) Comparative properties of cellulose nano-crystals from native and mercerized cotton fibers. Cellulose 19:1173–1187. https://doi.org/10.1007/s10570-012-9714-4

Zdanowicz M, Johansson C (2016) Mechanical and barrier properties of starch-based films plasticized with two- or three component deep eutectic solvents. Carbohydr Polym 151:103–112. https://doi.org/10.1016/j.carbpol.2016.05.061

Zhao G, Zhang Y, Zhai S, Sugiyama J, Pan M, Shi J, Lu H (2020) Dual response of photonic film with chiral nematic cellulose nanocrystal: humidity and formaldehyde. ACS Appl Mater Interfaces 12:17833–17844. https://doi.org/10.1021/acsami.0c00591

Zhu B, Merindol R, Benitez AJ, Wang B, Walther A (2016) Supramolecular engineering of hierarchically self-assembled, bioinspired, cholesteric nanocomposites formed by cellulose nanocrystals and polymers. ACS Appl Mater Interfaces 8(17):11031–11040. https://doi.org/10.1021/acsami.6b00410